

The model parameters  $P_a$  and  $\sigma$  were fitted to match the theoretical radius with the experimentally determined equivalent bubble radius of the ellipsoidal cavitation bubble (solid circles in Fig. 3). With these model parameters, the calculated sound pressure curve (from Eq. 3) is in good agreement with the experimental sound signal (Fig. 4). The main acoustical signal is preceded by a small sinusoidal precursor, caused by the bubble expansion and contraction. At collapse ( $t = 0$ ), the main acoustical signal is emitted. The narrow peaks in the calculated sound signal after the main pressure peak are produced by the aforementioned afterbounces and should not be considered here, as the bubble is destroyed on collapse. Quantitatively, the model overestimates the measured sound pressure, especially the maximum pressure, for three reasons: (i) The nonspherical shape of the real bubble reduces the strength of the collapse and therefore the intensity of the emitted sound, (ii) thermal damping effects (28) are not included in the model, and (iii) on the experimental side, the limited bandwidth of the hydrophone underestimates the peak value of the sound pressure.

The calculated width of the main acoustical peak for the modeled spherical bubble is very small, on the order of 100 ps. This  $\delta$ -like pulse corresponds to a white noise spectrum, consistent with the wide frequency range of the sound of the snapping shrimp. A more quantitative comparison of the theoretical and experimental spectrum must include the asphericity of the collapse, the acoustical emission of the bubble fragments, and the sound reflections from the walls into the model.

The variation in claw size, claw shape, cocking duration, applied closer muscle force, and claw closure speeds of snapping shrimp all lead to slightly different sound signals and have different water jet characteristics. By adjusting the parameters  $P_a$  and  $\sigma$  in our model, we are able to account for the variety of precursor signals measured in our experiments (29).

References and Notes

1. R. J. Urick, *Principles of Underwater Sound* (McGraw-Hill, New York, 1983).
2. D. H. Cato and M. J. Bell, *Material Research Laboratory Technical Report MRL-TR-91-23* (Defence Science and Technology Organisation, Sydney, Australia, 1992).
3. M. W. Johnson, F. A. Everest, R. W. Young, *Biol. Bull.* **93**, 122 (1947).
4. F. A. Everest, R. W. Young, M. W. Johnson, *J. Acoust. Soc. Am.* **20**, 137 (1948).
5. W. W. L. Au and K. Banks, *J. Acoust. Soc. Am.* **103**, 41 (1998).
6. B. Schmitz, in *The Crustacean Nervous System*, K. Wiese, Ed. (Springer-Verlag, Berlin, in press).
7. C. L. Epifanio, J. R. Potter, G. B. Deane, M. L. Readhead, M. J. Buckingham, *J. Acoust. Soc. Am.* **106**, 3211 (1999).
8. R. E. Ritzmann, *J. Comp. Physiol.* **95**, 217 (1974).
9. B. Schmitz and J. Herberholz, in *New Neuroethology on the Move, Proceedings of the 26th Göttingen Neurobiology Conference 1998*, vol. 2, N. Elsner and R. Wehner, Eds. (Thieme, Stuttgart, 1998), p. 241.

10. J. Herberholz and B. Schmitz, *J. Comp. Physiol. A* **185**, 41 (1999).
11. H. Schein, *Mar. Behav. Physiol.* **3**, 83 (1975).
12. J. Herberholz and B. Schmitz, *Biol. Bull.* **195**, 156 (1998).
13. G. E. MacGinitie and N. MacGinitie, *Natural History of Marine Animals* (McGraw-Hill, New York, 1949).
14. P. Volz, *Z. Morph. Oekol. Tiere* **34**, 272 (1938).
15. C. E. Brennen, *Cavitation and Bubble Dynamics* (Oxford Univ. Press, New York, 1995).
16. Video files of the snapping shrimp and links to audio files can be found at Science Online (available at [www.sciencemag.org/feature/data/1052273.shl](http://www.sciencemag.org/feature/data/1052273.shl)).
17. S. Schultz, K. Wuppermann, B. Schmitz, *Zool. Anal. Complex Syst.* **101** (suppl. I), 85 (1998).
18. J. R. Blake, Y. Tomita, R. P. Tong, *Appl. Sci. Res.* **58**, 77 (1998).
19. S. L. Ceccio and C. E. Brennen, *J. Fluid Mech.* **233**, 633 (1991).
20. A. Prosperetti and A. Lezzi, *J. Fluid Mech.* **168**, 457 (1986).
21. M. S. Plesset and A. Prosperetti, *Annu. Rev. Fluid Mech.* **9**, 145 (1977).
22. S. Hilgenfeldt, D. Lohse, M. Brenner, *Phys. Fluids* **8**, 2808 (1996).
23. B. D. Storey and A. J. Szeri, *Proc. R. Soc. London Ser. A* **456**, 1685 (2000).
24. R. Tögel, B. Gompf, R. Pecha, D. Lohse, *Phys. Rev. Lett.*, in press.
25. L. D. Landau and E. M. Lifshitz, *Fluid Mechanics* (Pergamon, Oxford, 1987).
26. S. Hilgenfeldt, D. Lohse, M. Zomack, *Eur. Phys. J. B* **4**, 247 (1998).
27. A. Prosperetti, *Q. Appl. Math.* **35**, 339 (1977).
28. Y. Hao and A. Prosperetti, *Phys. Fluids* **11**, 2008 (1999).
29. M. Versluis, B. Schmitz, A. von der Heydt, D. Lohse, in preparation.
30. W. K. Brooks and F. H. Herrick, *Mem. Natl. Acad. Sci. Wash.* **5**, 319 (1891).
31. This work was supported by a grant from the Stichting voor Fundamenteel Onderzoek der Materie (FOM) and by a grant from the Deutsche Forschungsgemeinschaft (Schn 693/5-4) to B.S. The experimental assistance of M. Hansbauer is gratefully acknowledged. We offer special thanks to N. Franz of the electronics workshop of the Department of Physics, Technical University of Munich, for repairing our Schmitt trigger device on Christmas Eve. M.V. is supported by FOM. A.H. is supported by the German-Israeli Foundation.

17 May 2000; accepted 20 July 2000

## Detecting and Measuring Cotranslational Protein Degradation in Vivo

Glenn C. Turner and Alexander Varshavsky\*

Nascent polypeptides emerging from the ribosome and not yet folded may at least transiently present degradation signals similar to those recognized by the ubiquitin system in misfolded proteins. The ubiquitin sandwich technique was used to detect and measure cotranslational protein degradation in living cells. More than 50 percent of nascent protein molecules bearing an amino-terminal degradation signal can be degraded cotranslationally, never reaching their mature size before their destruction by processive proteolysis. Thus, the folding of nascent proteins, including abnormal ones, may be in kinetic competition with pathways that target these proteins for degradation cotranslationally.

Nascent polypeptides emerging from the ribosome may, in the process of folding, present hydrophobic patches and other structural features that serve as degradation signals similar to those recognized by the ubiquitin (Ub) system in misfolded or otherwise damaged proteins (1). Whether a substantial fraction of nascent polypeptides is cotranslationally degraded is a long-standing question.

The Ub sandwich technique was developed to detect cotranslational protein degradation by measuring the steady-state ratio of two reporter proteins whose relative abundance is established cotranslationally. The technique requires that the polypeptide to be examined for cotranslational degradation, termed **B**, be sandwiched between two stable reporter domains, **A** and **C**, in a linear fusion

protein (Fig. 1A). The three polypeptides are connected by Ub moieties, creating an AUb-BUb-CUb fusion protein. Ub-specific processing proteases (UBPs) cotranslationally cleave such linear Ub fusions at the C-terminal residue of Ub (2-4), generating three independent polypeptides, AUb, BUb, and CUb (5). UBP-mediated cleavage establishes a kinetic competition between two mutually exclusive events during the synthesis of AUb-BUb-CUb: cotranslational UBP cleavage at the BUb-CUb junction to release the long-lived CUb module or, alternatively, cotranslational degradation of the entire BUb-CUb nascent chain by the proteasome (6) (Fig. 1B). In the latter case, the processivity of proteasome-mediated degradation results in the destruction of the Ub moiety between **B** and **C** before it can be recognized by UBPs. The resulting drop in levels of the CUb module relative to levels of AUb, referred to as the C/A ratio, reflects the cotranslational degradation of domain **B** (Fig. 1B).

Division of Biology, California Institute of Technology, Pasadena, CA 91125, USA.

\*To whom correspondence should be addressed. E-mail: [avarsh@caltech.edu](mailto:avarsh@caltech.edu)

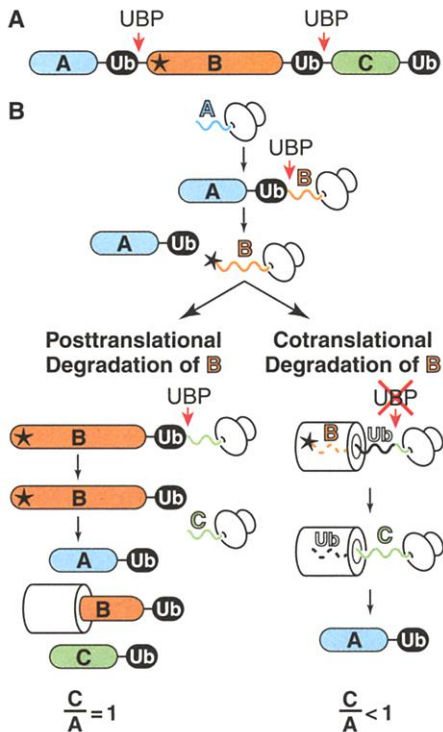


**Fig. 1.** The ubiquitin sandwich technique. (A) Organization of a Ub sandwich fusion. The polypeptide assayed for cotranslational degradation, B, is sandwiched between two stable reporter domains A and C. Red arrows indicate the locations of UBP cleavage sites. (B) The principle of the method. The reporter module AUb is the first synthesized and is cotranslationally released from B, thereby providing a measure of the number of nascent B chains that initially emerge from the ribosome. If degradation of the emerging B domain, indicated by its insertion into the proteasome, is strictly posttranslational, UBP-mediated cleavage at the BUB-C junction releases CUB before B is degraded, so the molar yields of CUB and AUB are identical. However, if degradation of B can be cotranslational, a substantial fraction of BUB-CUB may be degraded as a unit. This will result in the molar yield of CUB being lower than AUB, the difference being a measure of cotranslational degradation.

To verify that UBP-mediated cleavage is cotranslational (3), we carried out in vivo radiolabeling in which the labeling pulse was substantially shorter than the time required for the complete synthesis of AUb-BUB-CUB. *Saccharomyces cerevisiae* cells expressing the fusion protein {DHFRhaUb} - {Me<sup>K</sup>βgalUb} - {Me<sup>K</sup>DHFRhaUb} (Fig. 2A), predicted to require ~350 s for complete synthesis, were radiolabeled for 45 s (7). Labeling was terminated by addition of cycloheximide, and UBPs were simultaneously inactivated with *N*-ethylmaleimide (NEM) (3). Under these conditions, nascent chains that are just starting to be synthesized when the pulse begins will incorporate label into the N-terminal A domain but do not elongate to full-length chains (Fig. 2B). Thus,

**Fig. 2.** UBP-mediated cleavage of ubiquitin sandwich fusions is cotranslational. (A) The protein fusions used. Domains A and C are mouse dihydrofolate reductase tagged with the influenza hemagglutinin-derived ha epitope (DHFRha). Domain B carries an N-terminal extension (e<sup>K</sup>, see text), which makes it electrophoretically distinguishable from A. The different B domains are *E. coli* βGal, Sindbis virus RNA polymerase (nsP4), and *S. cerevisiae* Ura3p. Unstable versions of these domains have an N-terminal arginine (R) residue; stable versions have methionine (M). (B) The population of nascent chains produced by a radiolabeling pulse that is shorter than the time of translation of an AUB-BUB-CUB fusion. Stretches of polypeptide containing radiolabel are in red; unlabeled stretches are in black. If UBPs efficiently cleave the nascent chain, free radiolabeled AUB, BUB, and CUB should all be detected. If UBPs can cleave solely the full-length mature protein, only labeled CUB will be observed. (C) The UBP cleavage of Ub sandwich fusions is cotranslational. The release of AUB, BUB, and CUB by UBP cleavage was assayed by immunoprecipitation (7). CUB\* denotes both the Me<sup>K</sup>DHFRhaUb and a cross-reacting band present in these NEM-treated extracts but not in untreated ones (compare with Fig. 3A). M<sub>r</sub>, relative molecular mass.

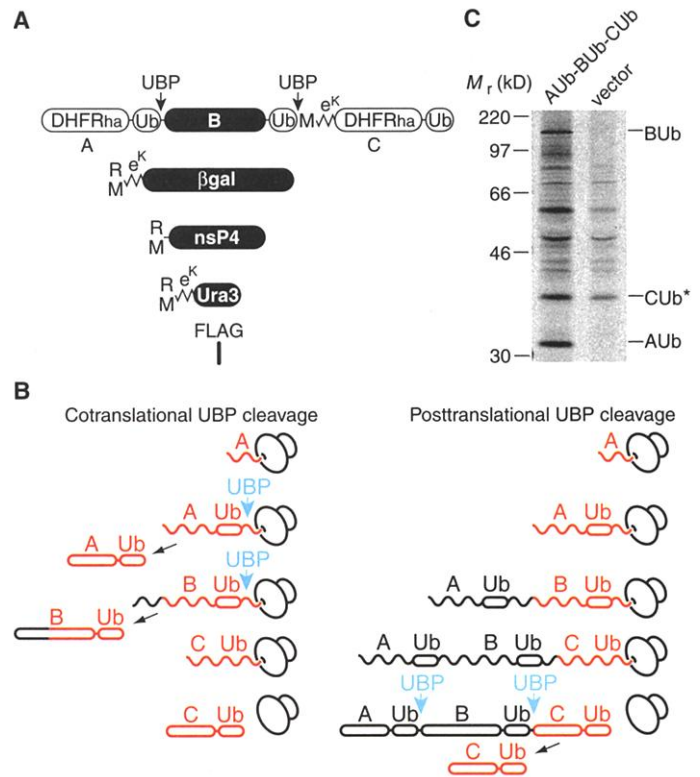
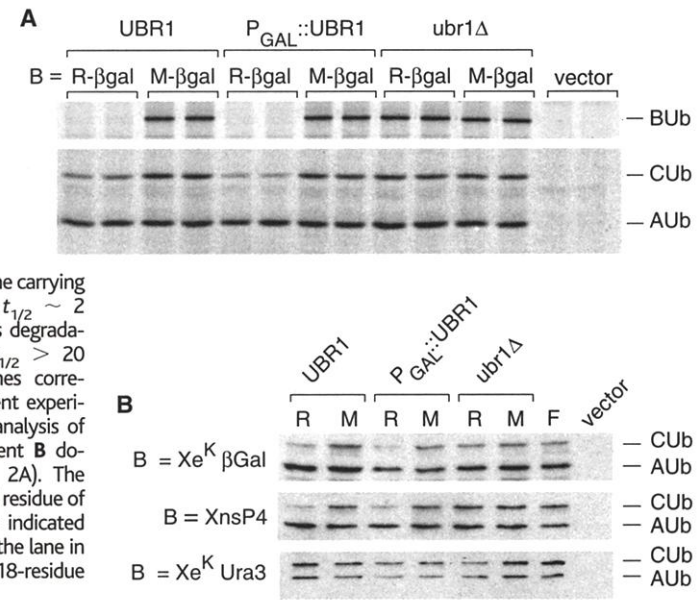


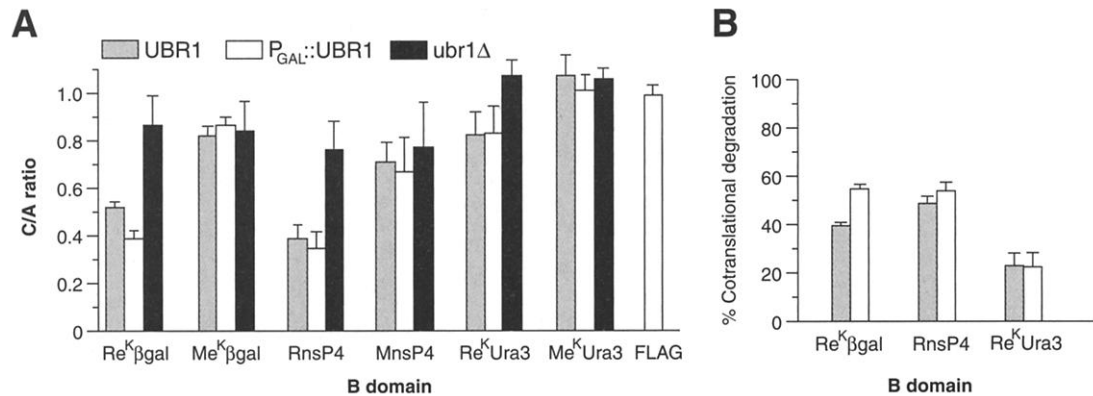
**Fig. 3.** Nascent polypeptides bearing an N-terminal degradation signal can be degraded cotranslationally. (A) Determination of C/A ratios through immunoprecipitation of in vivo-labeled AUb-BUB-CUB fusion proteins (14). Two variants of βgal were used as domain B, one carrying an N-degron (Re<sup>K</sup>-βgal; t<sub>1/2</sub> ~ 2 min) and one lacking this degradation signal (Me<sup>K</sup>-βgal; t<sub>1/2</sub> > 20 hours). Each pair of lanes corresponds to two independent experiments. (B) Immunoblot analysis of the C/A levels for different B domains (described in Fig. 2A). The identity of the N-terminal residue of each of the B domains is indicated above each lane. F marks the lane in which domain B was the 18-residue FLAG-containing moiety.



detection of free, labeled AUB and BUB by immunoprecipitation indicated that UBP-mediated cleavage at the AUb-BUB junction was cotranslational (Fig. 2C). No full-length AUb-BUB-CUB fusion was detected (Fig. 2C), indicating that cotranslational

cleavage by UBPs was highly efficient. Previous experiments bearing on cotranslational degradation used inhibitors or cell-free systems (8–10). Nascent polypeptide chains might be protected from degradation in vivo, either because they are sterically

**Fig. 4.** The extent of cotranslational protein degradation depends on the presence of a degron, the activity of a degron-specific proteolytic pathway, and the nature and size of the protein. **(A)** C/A ratios obtained for the different **B** domains. **(B)** Ubr1p-dependent cotranslational degradation (15). Each bar represents a mean value derived from at least four independent experiments; standard errors are indicated. Differences between means were significant to at least  $P < 0.05$  by the Mann-Whitney test. Bars are as in (A).



shielded by chaperones or because their translation time is short compared with the time required for targeting by the degradation machinery. The Ub sandwich technique was used to detect in vivo cotranslational degradation of a 118-kD, β-galactosidase (βgal)-derived polypeptide carrying a strong N-terminal degradation signal, specifically an N-degron (Fig. 2A). The βgal-linked N-degron comprises the destabilizing N-terminal residue arginine (R) and a short, lysine (K)-bearing extension, e<sup>K</sup> (Fig. 2A), that is the site of multi-Ub chain attachment (11). Ubr1p, the E3 component of the N-end rule pathway, targets Re<sup>K</sup>-βgal for rapid degradation in vivo [half-life ( $t_{1/2}$ ) ~ 2 min] (2, 12). Changing the N-terminal residue of the protein to methionine (M) inactivates the degradation signal by precluding recognition by Ubr1p. The resulting Me<sup>K</sup>-βgal is posttranslationally stable ( $t_{1/2} > 20$  hours) (2). AUb-BUb-CUb fusion proteins in which domain **B** was either Re<sup>K</sup>-βgal or its N-degron-lacking counterpart Me<sup>K</sup>-βgal (Fig. 2A) were expressed in *S. cerevisiae* strains containing different levels of Ubr1p (13). The extent of cotranslational degradation was assessed by radiolabeling for 30 min and immunoprecipitation (14) to determine the levels of CUb relative to AUb (the C/A ratio).

The C/A ratio was lower in cells expressing the N-degron-bearing domain **B**, but only in those strains that also expressed Ubr1p (Fig. 3A). To determine the percentage of nascent chains cotranslationally degraded by the N-end rule pathway, we compared the C/A ratios for Re<sup>K</sup>-βgal in wild-type (0.52) and Ubr1p-overexpressing strains (0.39) with the ratio found with the *ubr1Δ* strain (0.86) (Fig. 4A). This comparison indicated that ~40% of the nascent Re<sup>K</sup>-βgal chains were cotranslationally degraded in the wild-type strain (Fig. 4B) (15). This fraction increased to ~55% when Ubr1p was overexpressed from the P<sub>GAL1</sub> promoter.

The extent of cotranslational degradation of two other **B** domains of different sizes was also determined. The mammalian Sindbis virus

RNA polymerase, termed nsP4, is a 69-kD protein that naturally bears an N-degron (16), and Xe<sup>K</sup>-Ura3p (X = M or R) is a 34-kD enzyme of the *S. cerevisiae* uracil biosynthetic pathway that either carries (Re<sup>K</sup>-Ura3p) or lacks (Me<sup>K</sup>-Ura3p) an N-degron (17) (Fig. 2A). Although the short-lived R-nsP4 (69 kD) and Re<sup>K</sup>-βgal (118 kD) were cotranslationally degraded to similar extents, Re<sup>K</sup>-Ura3p (34 kD), which was also short-lived posttranslationally (17), exhibited much less cotranslational degradation than the other two proteins (Fig. 3B). Radiolabeling and immunoprecipitation (14) showed that ~50% of the nascent chains of R-nsP4 were cotranslationally degraded by the N-end rule pathway in wild-type cells and ~55% in cells overexpressing Ubr1p (Fig. 4B). These values were similar to ~40% and ~55% cotranslational degradation of Re<sup>K</sup>-βgal in these strains, respectively (Fig. 4B). In contrast, only ~20% cotranslational degradation was observed with the 34-kD Re<sup>K</sup>-Ura3p in either wild-type or Ubr1p-overexpressing strains (Fig. 4B). These results suggest that smaller proteins are less susceptible to cotranslational degradation; however, factors other than translation time likely influence the presentation or accessibility of the degradation signal by the nascent chain, because protein size was not directly proportional to the extent of cotranslational degradation.

These comparisons established the amounts of cotranslational degradation by the N-end rule pathway. The C/A ratios for two of the N-degron-lacking **B** domains, Me<sup>K</sup>-βgal (0.84) and M-nsP4 (0.72), were less than the C/A ratio obtained with a very short FLAG epitope-containing sequence that lacks a degradation signal and exhibits a C/A ratio of 0.97, indistinguishable from the theoretical value of 1.0 (Fig. 4A). This suggests that ~15% of Me<sup>K</sup>-βgal and ~25% of M-nsP4 nascent chains might be cotranslationally degraded by a Ubr1p-independent pathway. Premature termination of translation and/or transcription may also contribute to the drop in the C/A ratios for these **B** domains. However, it is unlikely that premature termination of translation accounts entirely for

the difference between the C/A ratios for FLAG and M-nsP4, because the codon adaptation index of the M-nsP4 open reading frame (0.1) is higher than the one for Me<sup>K</sup>-βgal (0.07), but the drop in C/A ratio is greater with M-nsP4 than with Me<sup>K</sup>-βgal. The degradation of newly synthesized polypeptides is a major source of peptides presented to the immune system (18, 19). Our observations with the above two **B** domains suggest that the source of these peptides is cotranslational protein degradation. In this regard, it is interesting that nsP4 is a viral protein that is presented efficiently to the immune system by infected cells.

The extent of cotranslational degradation can be strikingly high: In the case of Re<sup>K</sup>-βgal in Ubr1p-overexpressing cells, over 50% of nascent polypeptide chains never reach their full size before their destruction by processive proteolysis. Thus, if a nascent chain displays a degron of the Ub system, such a protein becomes a target of kinetic competition between cotranslational biogenesis and cotranslational degradation. Because the folding of a protein molecule begins during its synthesis on the ribosome, a nascent polypeptide may cotranslationally expose degradation signals that become shielded through the folding of the newly formed protein (20, 21). Thus, cotranslational protein degradation may represent a form of protein quality control that destroys nascent chains that fail to fold correctly rapidly enough.

**References and Notes**

1. A. Varshavsky, *Trends Biochem. Sci.* **22**, 383 (1997).
2. A. Bachmair, D. Finley, A. Varshavsky, *Science* **234**, 179 (1986).
3. N. Johnsson and A. Varshavsky, *EMBO J.* **13**, 2686 (1994).
4. F. Lévy, N. Johnsson, T. Rumenapf, A. Varshavsky, *Proc. Natl. Acad. Sci. U.S.A.* **93**, 4907 (1996).
5. The Ub moieties of the fusion protein serve as cleavage sites between domains **A**, **B**, and **C**. They do not target the attached protein for degradation (4), nor do they contribute to multi-Ub chain formation, because they carry a lysine to arginine substitution at position 48 (Ub<sup>R48</sup>) that prevents their conjugation to other Ub molecules at that position (11).
6. W. Baumeister, J. Walz, F. Zühl, E. Seemüller, *Cell* **92**, 367 (1998).
7. The expression of Ub sandwich proteins from the

$P_{GAL1}$  promoter on p426GAL1 vector (22) was induced with 0.1  $\mu$ M  $\beta$ -estradiol with a Gal4.ER.VP16 chimeric protein (23). Ten-milliliter cell cultures were harvested after 10 hours of induction (absorbance at 600 nm = 0.5 to 1) and labeled for 30 s with  $^{35}$ S-EXPRESS (0.7 mCi/ml; New England Nuclear). Cycloheximide and NEM (final concentrations of 0.5 mg/ml and 0.1 M, respectively) were then added, cell extracts were prepared from 0.2 ml of the resulting sample, and immunoprecipitations were carried out as described (17), with antibodies to ha (12CAs Boehringer),  $\beta$ gal (Promega), and/or FLAG (M2; Eastman Kodak), as appropriate. Total handling time to the beginning of cell lysis was 45 s. In the eukaryotic cell types examined, the rate of translation is 2 to 10 residues per second (24). Assuming a rate of five residues per second in *S. cerevisiae*, this pulse is seven times shorter than the duration of translation of the fusion protein. Immunoprecipitates were fractionated by 13% SDS-polyacrylamide gel electrophoresis, and band intensities were quantitated by PhosphorImager (Molecular Dynamics).

8. L. Lin, G. N. DeMartino, W. C. Greene, *Cell* **92**, 819 (1998).  
 9. W. Liao, S. C. J. Yeung, L. Chan, *J. Biol. Chem.* **273**, 27225 (1998).  
 10. S. Sato, C. L. Ward, R. R. Kopito, *J. Biol. Chem.* **273**, 7189 (1998).  
 11. V. Chau *et al.*, *Science* **243**, 1576 (1989).  
 12. A. Varshavsky, *Proc. Natl. Acad. Sci. U.S.A.* **93**, 12142 (1996).  
 13. The *S. cerevisiae* strains JD52 (*MATa lys2-801 ura3-52 trp1- $\Delta$ 63 his3- $\Delta$ 200 leu2-3,112*), JD54 (*P<sub>GAL1</sub>::UBR1*), and JD55 (*ubr1 $\Delta$* ) were described (17).  
 14. The procedure was as in (7), except that cells were labeled for 30 min with 0.11 mCi of  $^{35}$ S-EXPRESS, then pelleted, resuspended in 0.8 ml of ice-cold lysis buffer, and processed for immunoprecipitation (17).  
 15. For example, with Re<sup>K</sup>- $\beta$ gal, where C/A was 0.52 in wild-type cells and 0.86 in *ubr1 $\Delta$* , the level of the Ubr1p-dependent cotranslational degradation was  $100\% \times (1 - 0.52/0.86) = 40\%$ .  
 16. R. J. deGroot, T. Rumenapf, R. J. Kuhn, J. H. Strauss, *Proc. Natl. Acad. Sci. U.S.A.* **88**, 8967 (1991).

17. M. Ghislain, R. J. Dohmen, F. Lévy, A. Varshavsky, *EMBO J.* **15**, 4884 (1996).  
 18. E. A. J. Reits, J. C. Vos, M. Gromme, J. Neefjes, *Nature* **404**, 774 (2000).  
 19. U. Schuberg *et al.*, *Nature* **404**, 770 (2000).  
 20. J. Frydman and F. U. Hartl, *Science* **272**, 1497 (1996).  
 21. B. Bukau, E. Deuerling, C. Pfund, E. A. Craig, *Cell* **101**, 119 (2000).  
 22. D. Mumberg, R. Muller, M. Funk, *Nucleic Acids Res.* **22**, 5767 (1994).  
 23. J. F. Louvion, B. Havauxcopf, D. Picard, *Gene* **131**, 129 (1993).  
 24. A. S. Spirin, *Ribosome Structure and Protein Biosynthesis* (Cummings, Menlo Park, CA, 1986).  
 25. We thank F. Lévy and N. Johnsson for their contributions to early stages of this work and R. Deshaies, T. Iverson, T.-M. Yi, and members of the Varshavsky laboratory for helpful discussions and comments on the manuscript. This study was supported by a grant to A.V. from NIH. G.T. was supported in part by Amgen.

15 March 2000; accepted 31 July 2000

## A Function for Kinesin I in the Posterior Transport of *oskar* mRNA and Staufen Protein

Robert P. Brenda, Laura R. Serbus, Joseph B. Duffy, William M. Saxton\*

The asymmetric localization of messenger RNA (mRNA) and protein determinants plays an important role in the establishment of complex body plans. In *Drosophila* oocytes, the anterior localization of *bicoid* mRNA and the posterior localization of *oskar* mRNA are key events in establishing the anterior-posterior axis. Although the mechanisms that drive *bicoid* and *oskar* localization have been elusive, oocyte microtubules are known to be essential. Here we report that the plus end-directed microtubule motor kinesin I is required for the posterior localization of *oskar* mRNA and an associated protein, Staufen, but not for the anterior-posterior localization of other asymmetric factors. Thus, a complex containing *oskar* mRNA and Staufen may be transported along microtubules to the posterior pole by kinesin I.

The *Drosophila* oocyte provides an excellent model system for studies of how the localization of mRNAs helps to establish complex body plans (1, 2). During the late stages of oogenesis, *bicoid* (*bcd*) and *oskar* (*osk*) mRNAs are localized to the anterior and posterior poles of the oocyte, respectively. Subsequent localized expression of Bicoid protein is necessary for anterior patterning, whereas localized expression of Oskar is necessary for posterior patterning and germ cell development. Genes required for the localization of *bcd* mRNA (e.g., *exuperantia* and *swallow*) and *osk* mRNA (e.g., *staufen* and *orb*) have been identified (1, 2), but the mechanisms of localization are not well understood.

Before stage 7 of oogenesis, the oocyte nucleus and a microtubule organizing center

(MTOC) are positioned at the posterior pole, generating a high concentration of microtubule minus ends near the posterior cortex (3–6). During stages 7 and 8, MTOC components switch to the anterior end, resulting in the reorganization of microtubules to place plus ends toward the posterior cortex (3–6). The oocyte nucleus then migrates from the posterior to the anterior end in a microtubule-dependent manner (1, 2, 7).

The localization of *bcd* and *osk* mRNAs between stages 8 and 12 is sensitive to microtubule-depolymerizing drugs, consistent with active transport of the mRNAs along microtubules by motor proteins (5, 8, 9). According to this model, *bcd* is moved to the anterior cortex by minus end-directed motors, such as dyneins, and *osk* is moved to the posterior cortex by plus end-directed motors, such as kinesins. Indeed, a dynein light chain can bind directly to Swallow, a putative RNA-binding protein necessary for anterior *bcd* localization (10).

If *osk* is transported to the posterior pole along microtubules, one or more of the more than 20 *Drosophila* kinesin superfamily members (11) might drive the movement. We focused our attention on *Kinesin heavy chain* (*Khc*) and its encoded protein KHC. KHC is the force-producing subunit of the tetrameric adenosine triphosphatase kinesin I (conventional kinesin), which in *Drosophila* and other metazoan animals serves as a motor for plus end-directed fast axonal transport of membranous organelles (12).

To determine if kinesin I is involved in oocyte patterning, we used mitotic recombination to generate mosaic female flies that contained clones of homozygous *Khc* null germ line stem cells (13–16). Western blots confirmed the depletion of KHC in embryos produced from such germ line clones (Fig. 1) (17). The production of eggs and embryos by the mosaic females suggests that germ line stem cells can proliferate and proceed through oogenesis without kinesin I. However, embryogenesis failed, despite fertilization by wild-type males. Most embryos arrested before blastoderm formation, but a few proceeded into early gastrulation stages. This maternal lethal effect was completely rescued by a wild-type *Khc* transgene (14, 18). Thus, germ line expression of KHC was required for normal embryogenesis, contrary to previous results from studies of a hypomorphic temperature-sensitive *Khc* allele (13).

Examination of embryos that reached the blastoderm stage revealed an absence of pole cells, the germ line precursors. To assay for earlier defects, we examined the distributions of *osk* and *bcd* mRNAs in *Khc* null oocytes (19). The localization of *bcd* mRNA was normal (Fig. 2, A and B), concentrated at the anterior during stages 8 to 10 (193 observed). In contrast, the localization of *osk* mRNA was defective (Fig. 2, C to F). It normally accumulates transiently at the anterior pole early in stage 8 and then moves to the poste-

Department of Biology, Indiana University, Bloomington, IN 47405, USA.

\*To whom correspondence should be addressed. E-mail: bsaxton@bio.indiana.edu